Journal of Solid State Chemistry 183 (2010) 3086–3092

Contents lists available at ScienceDirect

Journal of Solid State Chemistry

journal homepage: www.elsevier.com/locate/jssc

The adsorption of 1,3-butadiene on Pd/Ni multilayers: The interplay between spin polarization and chemisorption strength

Guillermina Gómez [a], Patricia G. Belelli [b,*], Gabriela F. Cabeza [b], Norberto J. Castellani [b]

[a] Grupo de Materiales y Sistemas Catalíticos, Departamento de Física, Universidad Nacional del Sur, Av. Alem 1253, Bahía Blanca B8000CPB, Argentina
[b] CONICET, Argentina

ARTICLE INFO

Article history:
Received 29 March 2010
Received in revised form
7 October 2010
Accepted 16 October 2010
Available online 4 November 2010

Keywords:
1,3-butadiene adsorption
Pd/Ni multilayers
Magnetism
Electronic structure
DFT

ABSTRACT

The adsorption of 1,3-butadiene (BD) on the Pd/Ni(1 1 1) multilayers has been studied using the VASP method in the framework of the density functional theory (DFT). The adsorption on two different configurations of the Pd_n/Ni_m(1 1 1) systems were considered. The most stable adsorption sites are dependent on the substrate composition and on the inclusion or not of spin polarization. On Pd_1Ni_3(1 1 1) surface, di–π–cis and 1,2,3,4-tetra-σ adsorption structures are the most stable for non-spin polarized (NSP) and spin polarized (SP) levels of calculation, respectively. Conversely, on Pd_3Ni_1(1 1 1) surface, the 1,2,3,4-tetra-σ adsorption structure is the most stable for both NSP and SP levels, respectively. The magnetization of the Pd atoms strongly modifies the adsorption energy of BD and its most stable adsorption mode. On the other hand, as a consequence of BD adsorption, the Pd magnetization decreases. The smaller adsorption energies of BD and 1-butene on the Pd_1Ni_3(1 1 1) surface than on Pd(1 1 1) can be associated to the strained Pd overlayer deposited on Ni(1 1 1).

1. Introduction

The selective hydrogenation of unsaturated hydrocarbons is an essential process in many chemical industries, such as pharmaceuticals, food additives, flavors and fragrances, and agrochemicals [1,2]. An example of such role is the complete elimination of dienes and alkynes from alkene feedstocks used in polymerization reactions. Besides, the selective hydrogenation of edible oil is also desirable to obtain the corresponding *cis*-fatty acids or the selective hydrogenation of carbon–carbon double bonds in presence of other functional groups [3–6].

The 1,3-butadiene molecule (BD) is the simplest conjugated hydrocarbon and can be used as a model to understand the chemical reactivity of more complicated hydrocarbons on metallic surfaces. The activity of BD hydrogenation on Ni(1 1 1) is very poor [7], but on Pd(1 1 1) this reaction is highly selective to obtain the partial hydrogenated product [8,9] and less selective and with poor activity on Pt(1 1 1) [10,11]. UPS and NEXAFS experiments showed that at low temperatures BD is loosely bonded to Pt and Pd, but at room temperature a strong chemisorption is produced [10,12]. For Pt(1 1 1) and Pd(1 1 1) surfaces, the di-σ and the di-π adsorption sites were proposed as the most favoured, respectively. However, the same 1,2,3,4-tetra-σ adsorption mode was theoretically found on both metal surfaces, with similar adsorption energies [13,14].

The activity and selectivity of BD hydrogenation strongly depends on the transition metal used as catalyst. Palladium is the most active and selective for this reaction, but these properties can be improved by changing the structure of the catalytic particle or by alloying it with another transition metal [15–18]. Bimetallic catalysts as Pd/Ni were employed for these reactions with a notorious catalytic performance [19,20]. In order to have a more precise idea of the nature of the catalytic active sites involved in this reaction, several UHV experiments on model surfaces have been performed. A multi-technique characterization of Pd/Ni overlayers including LEED, LEIS, EDS, TEM, and different electron spectroscopies indicated that such systems present better performance for BD hydrogenation than the pure Pd catalyst [12,21]. The analysis of the local geometry by the EXAFS technique is consistent with the production of a compressively stressed top layer of Pd atoms. Owing to the larger atomic radius of Pd (nearly 10%) compared with Ni, the surface of this bimetallic system undergoes rearrangements in UHV [22,23]. On the other hand, ultra-thin palladium films deposited on the Ni(1 1 1) surface were characterized by LEED, XPS, and XPD [24,25]. XPS and angle-resolved XPS measurements demonstrated that at room temperature Pd grows in a layer-by-layer mode over the Ni(1 1 1) surface, covering with islands the majority of the surface after annealing.

From the theoretical point of view, scarce investigations were realized. An earlier work for the BD adsorption on Pd(1 1 1) and Pd/Ni(1 1 1) based on the extended Hückel method [26] predicted a higher adsorption strength for the pure metal surface in comparison with the bimetallic system. Recently, the same research group has

* Corresponding author. Fax: +54 291 4595142.
E-mail address: pbelelli@plapiqui.edu.ar (P.G. Belelli).

0022-4596/$ - see front matter © 2010 Elsevier Inc. All rights reserved.
doi:10.1016/j.jssc.2010.10.022

studied the ethylene hydrogenation on a nano-structured catalyst constituted by a four monolayer deposit of Pd on Ni(1 1 0) [27]. In this case, the calculated activation energies showed that the Pd/Ni(1 1 0) surface is more active than pure Pd(1 1 0) surface.

In the last years, the magnetic properties of TM bimetallic systems where one of the metals presents ferromagnetic ordering as pure component have been the subject of interest. Thus, theoretical and experimental works have been performed to evaluate the magnetic properties of ordered alloys of $M_{1-x}Pd_x$, where M represents Co or Ni [28,29]. For a FCC stacking layered structure, the Pd atoms are strongly spin polarized while the magnetic moments of Ni and Co are significantly enhanced on alloys in comparison with the pure metal components. On the other hand, the theoretical study of the geometrical structure of the Pd_8Ni_{92}(1 1 0) alloy surface, where a complex "sawtooth" (ST) reconstruction has been observed, depends crucially on the inclusion of spin-polarization effects [30]. Very recently it has been predicted that in Pd–Ni multilayers the Pd atoms are strongly polarized when they are compared with pure Pd(1 1 1) and that the magnetic moment of Pd atoms increases according with the number of Pd layers [31]. Particularly, the calculated average magnetic moments are in agreement with recent experimental results [29].

In the present work, we investigate the binding site preference and the adsorption energies of BD on two multilayer surface models: Pd_1Ni_3(1 1 1) and Pd_3Ni_1(1 1 1), taking into account the ferromagnetic condition acquired by the Pd overlayer epitaxially deposited on the Ni(1 1 1) surface [31]. The goal is to analyze any possible interplay between spin polarization and chemisorption strength. In this sense and to analyze such effects both spin polarization (SP) and non-spin polarization (NSP) levels of calculation have been considered. To our knowledge, non-spin polarized results were reported in the past for these systems.

2. Theoretical details

All calculations reported in this work were carried out in the framework of DFT using the Vienna Ab-initio Simulation Program (VASP) [32–34]. In this code plane wave basis sets are used to solve the Kohn–Sham equations. Electron exchange and correlation effects are described by the generalized gradient approximation (GGA) using the functional proposed by Perdew–Wang (PW91) [35,36]. The electron–ion interactions are described by the projector-augmented wave (PAW) potentials. The PAW method is a frozen core all-electron method that uses the exact shape of the valence wavefunctions instead of pseudo-wave functions [37,38].

The fixed convergence of the plane-wave expansion was obtained with a cut-off energy of 450 eV. This value is based on our previous tests, which showed that the converged calculation error was lower than 0.01 eV. The two dimensional Brillouin integrations were fulfilled on a $(3\times3\times1)$ Monkhorst-Pack grid [39]. The ground state was obtained using a Methfessel-Paxton smearing of 0.2 eV [40]. In order to evaluate the magnetic properties of the systems, the calculations were performed at the SP and NSP levels.

For all the calculations, a FCC stacking layered structure was assumed. The (1 1 1) metallic surface was represented with a slab containing four layers of atoms separated in the normal direction by a vacuum region. The width of this gap was optimized to avoid the interaction between slabs. For that purpose, we observed that a distance of $\sim$15 Å is adequate to eliminate the interaction between adjacent metal slabs. The configuration used for the multilayers were of the type Pd_n/Ni_m(1 1 1) where n Pd layers are piled up over m Ni layers ($n=1$ or 3 with $n+m=4$). In this work, the BD molecule was adsorbed on different adsorption sites of two bimetallic surfaces: Pd_1Ni_3 and Pd_3Ni_1. The electronic and magnetic properties of these Pd/Ni multilayer materials were previously analyzed [31]. In order to minimize the interaction between adsorbates, a (3×3) super-cell was used. The adsorbate species was placed in one side of the slab and its geometry was allowed to optimize completely together with the two uppermost layers of the slab. The adsorption energy (E_{ads}) was calculated as the difference between the energy of the adsorbed molecule ($E_{adsorbate\text{-}surface}$) and the sum of the free surface ($E_{surface}$) and the gas-phase molecule ($E_{gas\text{-}phase}$) energies. A negative value indicates an exothermic chemisorption process. A large box of $(20\times20\times20)$ Å^3 was used to obtain the gas-phase molecule energy. The internal geometry was in agreement with previous theoretical results [14].

Some electronic characteristics as the local density of orbital states (LDOS), the change in the work function ($\Delta\Phi$) and the change of the dipole moment ($\Delta\mu$) were evaluated. $\Delta\Phi$ was calculated as the difference between the work function of the surface with and without adsorbed molecule and $\Delta\mu$ was analyzed considering different contributions [41].

3. Results and discussion

3.1. Adsorption of BD on Pd/Ni surfaces

Different adsorption modes for BD on Pd/Ni were considered, in all cases with the two C=C double bonds interacting with the bimetallic surface. Specifically, they are: di-π-cis, di-π-trans, 1,2,3,4-tetra-σ, 1,2-di-σ-3,4-π and 1,4-di-σ-2,3-π modes (Fig. 1). The differences between them reside on the number of Pd atoms with which interacts each C atom belonging to the double bonds, i.e., one (π) or two (di-σ) Pd atoms. In Tables 1 and 2, the equilibrium interatomic distances and the adsorption energies for BD adsorbed on different sites of Pd_1Ni_3(1 1 1) and Pd_3Ni_1(1 1 1) multilayers are summarized, respectively. The corresponding geometries show an elongation of the C=C double bonds (C_1C_2 and C_3C_4) with respect to the gas phase molecule (1.34 Å), while the C–C single bond remains almost unchanged (1.45 Å). The former stretching is more pronounced for the di-σ adsorption modes. Only in the case of the 1,4-di-σ-2,3-π adsorption mode, the central C–C single bond of the adsorbed diene is shortened. The internal geometry of molecule does not change significantly with the substrate, independently of the level (NSP or SP) carried out in the calculation. On the other hand, the Pd–C distances depend both on the adsorption site and the substrate. For the same bimetallic surface, the Pd–C bonds are longer at the SP level. This behavior can be associated with the lower surface relaxation with the BD adsorption at SP level, as it will be explained later. Comparing both bimetallic surfaces, we found that the Pd–C distances are in general longer on Pd_1Ni_3(1 1 1) than on Pd_3Ni_1(1 1 1). Evidently, in the last surface the Pd–Pd distances are less contracted (2.76 Å) than in Pd_1Ni_3(1 1 1) (2.57 Å), both with respect to the pure Pd(1 1 1) surface value (2.81 Å). This fact improves the molecule anchoring on Pd_3Ni_1(1 1 1) due to its relatively more open structure. Besides, the strain suffered by Pd atoms in the last system is smaller than that in the case of one monolayer of Pd deposited epitaxially on Ni(1 1 1).

On the other hand, an expansion of both Δd_{12} and Δd_{23} interlayer distances were observed for Pd_1Ni_3(1 1 1) as well for Pd_3Ni_1(1 1 1); though the change of Δd_{23} interlayer distances are not higher than 0.3% with respect to the bare surfaces. At the same level of calculation, the adsorption of BD produces a greater surface relaxation on Pd_1Ni_3(1 1 1) than on Pd_3Ni_1(1 1 1). The Δd_{12} interlayer distance increases up to 5%, for the di-π-cis adsorption mode on Pd_1Ni_3(1 1 1) at the NSP level, while the expansion is much reduced at the SP level (up to 2.5%). These results indicate that the

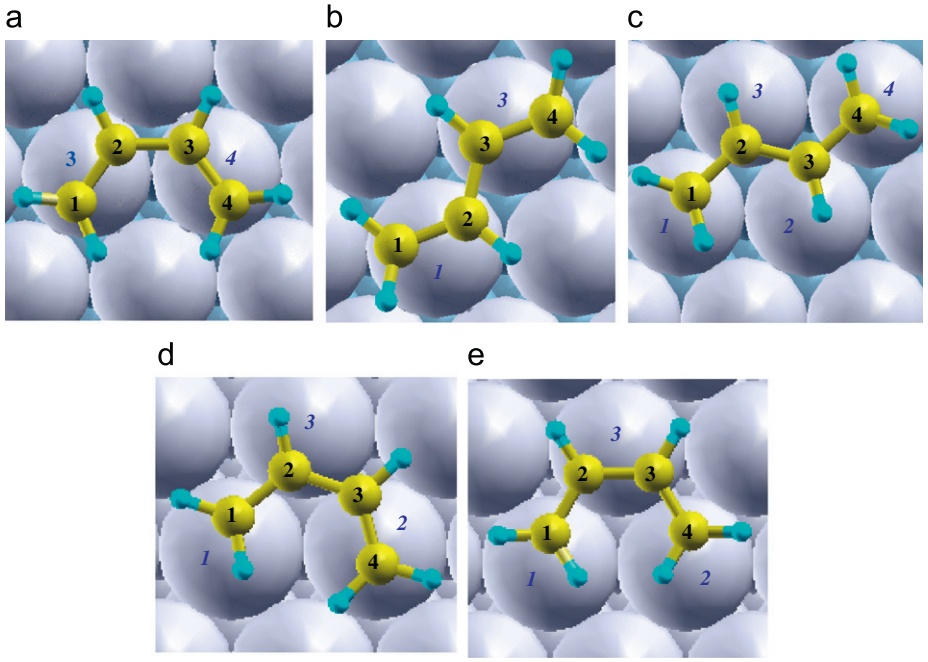

Fig. 1. Adsorption sites for 1,3-butadiene on Pd_1Ni_3(1 1 1) and Pd_3Ni_1(1 1 1) surfaces: (a) di-π-cis, (b) di-π-trans, (c) 1,2,3,4-tetra-σ, (d) 1,2-di-σ-3,4-π and (e) 1,4-di-σ-2,3-π. The corresponding Pd atoms are indicated by the cursive and blue color numbers. (For interpretation of the references to color in this figure legend, the reader is referred to the web version of this article.)

Table 1
Adsorption energies (eV) and geometric parameters for the optimized structures of 1,3-butadiene on Pd_1Ni_3(1 1 1) surface. For butene isomers, only the di-σ adsorption modes were listed.

Level	Adsorption site	E_{ads}	C_1C_2	C_2C_3	C_3C_4	C_1Pd	C_2Pd	C_3Pd	C_4Pd
NSP	di-π-cis	−0.72	1.41	1.46	1.42	2.15	2.23	2.22	2.16
	di-π-trans	−0.66	1.41	1.45	1.41	2.19	2.22	2.21	2.20
	1,2,3,4-tetra-σ	−0.68	1.44	1.44	1.43	2.15	2.34	2.41	2.15
	1,2-di-σ-3,4π	−0.57	1.44	1.44	1.41	2.14	2.25	2.39	2.19
	1,4-di-σ-2,3π	−0.62	1.45	1.43	1.45	2.14	2.26	2.27	2.15
	1-butene	−0.46	1.45	1.51	1.54	2.13	2.16	2.95	4.37
	cis-2-butene	−0.35	1.51	1.45	1.52	2.98	2.17	2.16	2.98
	trans-2-butene	−0.32	1.52	1.46	1.51	2.92	2.15	2.15	2.97
SP	di-π-cis	−0.42	1.41	1.46	1.41	2.20	2.28	2.27	2.21
	di-π-trans	−0.44	1.40	1.45	1.40	2.21	2.23	2.22	2.24
	1,2,3,4-tetra-σ	−0.52	1.43	1.43	1.43	2.16	2.34	2.43	2.16
	1,2-di-σ-3,4π	−0.38	1.44	1.45	1.41	2.17	2.27	2.42	2.22
	1,4-di-σ-2,3π	−0.43	1.44	1.43	1.44	2.15	2.28	2.30	2.16
	1-butene	−0.33	1.44	1.51	1.54	2.15	2.18	2.95	4.38
	cis-2-butene	−0.25	1.51	1.45	1.51	2.99	2.18	2.19	2.99
	trans-2-butene	−0.15	1.52	1.45	1.52	2.94	2.17	2.16	2.97

Table 2
Adsorption energies (eV) and geometric parameters for the optimized structures of 1,3-butadiene on Pd_3Ni_1(1 1 1) surface. For butene isomers, only the di-σ adsorption modes were listed.

Level	Adsorption site	E_{ads}	C_1C_2	C_2C_3	C_3C_4	C_1Pd	C_2Pd	C_3Pd	C_4Pd
NSP	di-π-cis	−1.20	1.41	1.46	1.41	2.16	2.26	2.24	2.16
	di-π-trans	−1.16	1.41	1.46	1.42	2.19	2.23	2.15	2.29
	1,2,3,4-tetra-σ	−1.52	1.45	1.45	1.44	2.12	2.23	2.29	2.11
	1,2-di-σ-3,4π	−1.35	1.45	1.45	1.42	2.12	2.18	2.36	2.15
	1,4-di-σ-2,3π	−1.39	1.45	1.43	1.45	2.11	2.26	2.25	2.11
	1-butene	−0.81	1.45	1.52	1.54	2.12	2.15	2.96	4.84
	cis-2-butene	−0.75	1.51	1.46	1.51	2.95	2.14	2.14	2.94
	trans-2-butene	−0.69	1.52	1.46	1.51	2.95	2.14	2.12	2.95
SP	di-π-cis	−1.16	1.41	1.46	1.41	2.16	2.27	2.24	2.17
	di-π-trans	−1.14	1.41	1.46	1.41	2.19	2.24	2.17	2.29
	1,2,3,4-tetra-σ	−1.49	1.45	1.45	1.44	2.12	2.23	2.29	2.11
	1,2-di-σ-3,4π	−1.32	1.46	1.45	1.42	2.11	2.18	2.37	2.15
	1,4-di-σ-2,3π	−1.35	1.45	1.43	1.45	2.11	2.27	2.26	2.11
	1-butene	−0.77	1.45	1.52	1.54	2.13	2.17	2.96	4.42
	cis-2-butene	−0.68	1.51	1.46	1.51	2.95	2.15	2.14	2.93
	trans-2-butene	−0.57	1.52	1.47	1.51	2.95	2.14	2.12	2.95

interaction of the Pd monolayer with the Ni substrate is higher when the calculations are performed at SP level [31].

For the Pd_1Ni_3(1 1 1) surface, the di-π-cis and 1,2,3,4-tetra-σ adsorption modes are the most stables at NSP and SP levels, respectively. The adsorption energies of the remaining sites, evaluated with NSP and SP, decrease about ∼0.15 eV in magnitude with respect to the most stable adsorption site. In all cases, the SP level gives adsorption energies nearly 0.2 eV lower in magnitude than the NSP level. Extended-Hückel calculations using a Pd_7-in-Ni(1 1 1) embedded cluster model showed the di-π-cis as the adsorption mode with better stability (−0.65 eV) [26]. This result is 10% lower than our NSP calculations on Pd_1Ni_3(1 1 1). Notice that the magnitude of BD adsorption energies are higher on Pd_3Ni_1(1 1 1) than on Pd_1Ni_3(1 1 1) and, concomitantly, the Pd–C bonds are shorter. On the former surface, the 1,2,3,4-tetra-σ adsorption site is preferred at both NSP and SP levels. The adsorption energies of remaining sites decrease up to ∼0.35 eV in magnitude with respect to the most stable adsorption site. From previous theoretical studies on Pt(1 1 1) and Pd(1 1 1) surfaces performed at the NSP level, the 1,2,3,4-tetra-σ site was found as the most stable adsorption mode for BD [13,14]. This result was the same as that reported here for Pd_3Ni_1(1 1 1) (NSP). It can be viewed as reasonably taking into account that the Pd_3Ni_1(1 1 1) surface is electronically similar to Pd(1 1 1) [31]. The adsorption energy difference between them is of 0.2 eV, being the monometallic surface the most stable for BD.

Analyzing the effect of the NSP and SP approaches we notice that when the spin polarization is taken into consideration, the system containing the higher proportion of ferromagnetic component undergoes the larger modifications. The most stable adsorption

mode of BD on Pd_1Ni_3(1 1 1) changes accordingly to the theoretical approach (NSP/SP); its binding energy and the energy difference with respect to the second most stable adsorption site also change. In particular, the E_{ads} differences between the first and the second most stable adsorption sites for NSP and SP are 5.5% and 15.5%. For Pd_3Ni_1(1 1 1), the same adsorption mode was obtained for both NSP and SP levels and the energy differences between the first and the second most stable adsorption sites are practically the same (8.5% and 9.4% for NSP and SP). It is appropriate to mention that, for comparison reason, the NSP and SP calculations have not been performed on a pure Pd(1 1 1) because the spin polarization effect is null in a metallic surface with non-magnetic element. This issue was carefully checked performing some BD adsorptions on the Pd(1 1 1) surface and their adsorption energies, geometries and magnetic moments are equivalent as those previously reported with non-spin polarized calculations [13,14].

In Table 3 the magnetic moments (mm) of interacting C and Pd atoms for Pd_1Ni_3 and Pd_3Ni_1 are summarized. In all cases, no magnetic moment for C atoms of BD are obtained. Conversely, the mm of interacting Pd atoms decrease at least 60% with respect to the clean surface. For Pd_1Ni_3(1 1 1), the mm values of interacting Pd atoms decrease in the same direction that adsorptions are stabilized. In Fig. 2a this behavior is clearly illustrated, where the mm values of interacting Pd atoms and that of the whole layer of Pd atoms decrease as the stabilization of the site increase, i.e., the 1,2,3,4-tetra-σ adsorption site has the surface Pd atoms with lowest mm value and it presents the better stability. The Pd_3Ni_1 (1 1 1) surface shows an equivalent behavior, but in this case the mm values are twice higher than on Pd_1Ni_3(1 1 1) (see Fig. 2b). Notice that the mm value for clean Pd_3Ni_1(1 1 1) surface is also twice higher than for Pd_1Ni_3(1 1 1); however, in the former system, for which we have the greater diene adsorption energies, we have also greater changes of the mm values of Pd atoms. It seems that the physical origin of this electron pairing enhancement is the same for both surfaces and it is intimately related to the chemisorptive bonding of BD. Similar results have been obtained theoretically for the adsorption of CO on Ni(1 1 0) [42] and experimentally for CO linked to small Ni unsupported clusters [43].

The work function change ($\Delta\Phi$) is directly associated with the change of the electric dipole in the surface after the molecular adsorption. The electron donation from molecule to metal is expected to decrease the work function, whereas the back-donation from the metal to adsorbate increases this property. Consequently, metals with positive $\Delta\Phi$ upon adsorption are characterized by a strong back-donation that over-compensates the electron donation, leading to a positive dipole moment. Evaluating the $\Delta\Phi$ upon the BD chemisorption with respect to the clean surface, we observe that in all the cases negative values are obtained (Table 4). The dipole moment change ($\Delta\mu$), generated by the BD on the bimetallic surface, generates an easier extraction of the electron from the bulk. The $\Delta\Phi$ values present a small variation in a range 1.12–1.35 eV, indicating poor dependence on the adsorption sites and on the substrate surfaces. Experimental results of CO adsorbed on Pd/Cu alloys with different compositions showed the sensibility of the $\Delta\Phi$ to determine the top layer composition of alloys [44], but as our Pd/Ni surfaces contain only Pd atoms in the top layer no such degree of sensibility to the surface composition could be expected.

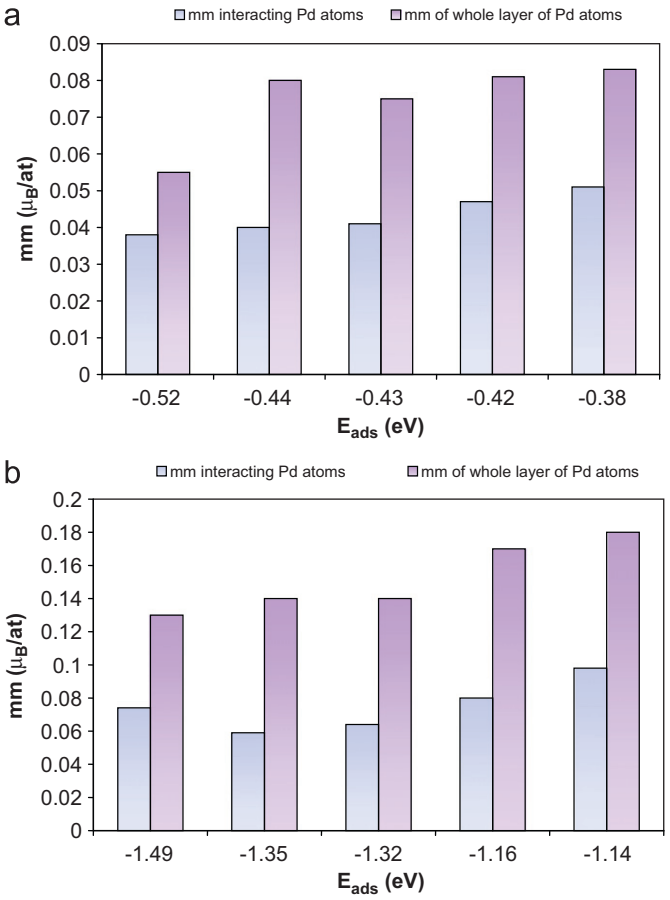

Fig. 2. Magnetic moments (mm) of Pd atoms on: (a) Pd_1Ni_3(1 1 1) and (b) Pd_3Ni_1(1 1 1) surfaces interacting with 1,3-butadiene as a function of adsorption energies (E_{ads}) for the different sites presented in Tables 1 and 2.

Table 3
Magnetic moments (μ_B/atom) for the 1,3-butadiene adsorbed molecule and the interacting Pd atoms obtained by the SP calculations. The mm of the Pd atoms interacting with C atoms are remarked using **bold** characters.

Atom	di-π-cis	di-π-trans	1,2,3,4-tetra-σ	1,2-di-σ-3,4π	1,4-di-σ-2,3π
Pd_1Ni_3 (0.129) [a]					
Pd_1	0.086	**0.042**	**0.028**	**0.047**	**0.044**
Pd_2	0.086	0.094	**0.048**	**0.062**	**0.044**
Pd_3	**0.047**	**0.037**	**0.043**	**0.053**	**0.036**
Pd_4	**0.046**	0.089	**0.031**	0.101	0.099
Pd_3Ni_1 (0.282) [a]					
Pd_1	0.204	**0.104**	**0.069**	**0.061**	**0.060**
Pd_2	0.206	0.211	**0.083**	**0.057**	**0.059**
Pd_3	**0.079**	**0.099**	**0.081**	**0.073**	**0.057**
Pd_4	**0.080**	0.218	**0.065**	0.192	0.192

[a] The mm for clean surfaces are shown between parenthesis.

In other to understand these results, the dipolar moment contributions were also evaluated and included in Table 4. The $\Delta\mu$ is the result of two contributions: that from the individual BD molecules ($\mu_{1,3but}$) and that from the charge reordering after the chemisorption (μ_{transf}) [41]. Taking into account that the coverage was maintained fixed in all the cases equal to 1/9, the value of $\Delta\mu$ as well as the $\Delta\Phi$ can be considered as intensive properties expressed per unit adsorbed molecule. The values of $\mu_{1,3but}$ were calculated considering the geometry of the adsorbed molecule in each case without the presence of the metal surface. The distortions of the molecule generated important $\mu_{1,3but}$ values that are dependent on the adsorption site. From these values it is possible to identify that the smaller deformation occurs for the di-π-trans adsorption mode on both surfaces and that the bigger distortions take place in the 1,4-di-σ-2,3π site on Pd_1Ni_3(1 1 1) surface and in the 1,2,3,4-tetra-σ site on Pd_3Ni_1(1 1 1) surface. In general, the distortions undergone by the diene are bigger when the molecule is adsorbed on

Table 4
Work function changes ($\Delta\Phi$ in eV), dipole moment changes ($\Delta\mu$ in Debye), dipole moment of distorted 1,3-butadiene ($\mu_{1,3but}$ in Debye) and dipole moment due to the charge transfer (μ_{transf} in Debye) of 1,3-butadiene adsorbed in different modes on Pd_1Ni_3(1 1 1) and Pd_3Ni_1(1 1 1) for NSP and SP levels.

Slab	Adsorption site	NSP				SP			
		$\Delta\Phi$	$\Delta\mu$	$\mu_{1,3but}$	μ_{transf}	$\Delta\Phi$	$\Delta\mu$	$\mu_{1,3but}$	μ_{transf}
Pd_1Ni_3	di-π-cis	−1.23	−1.71	−0.71	−1.00	−1.31	−1.70	−0.64	−1.06
	di-π-trans	−1.27	−1.82	−0.67	−1.14	−1.32	−1.71	−0.58	−1.13
	1,2,3,4-tetra-σ	−1.21	−1.68	−0.99	−0.69	−1.27	−1.62	−0.93	−0.69
	1,2-di-σ-3,4π	−1.19	−1.66	−0.92	−0.73	−1.28	−1.63	−0.85	−0.79
	1,4-di-σ-2,3π	−1.33	−1.97	−1.05	−0.92	−1.23	−1.61	−0.99	−0.62
Pd_3Ni_1	di-π-cis	−1.23	−1.90	−0.80	−1.10	−1.32	−2.03	−0.77	−1.26
	di-π-trans	−1.16	−1.84	−0.81	−1.03	−1.35	−2.08	−0.75	−1.33
	1,2,3,4-tetra-σ	−1.12	−1.75	−1.21	−0.54	−1.23	−1.90	−1.15	−0.75
	1,2-di-σ-3,4π	−1.19	−1.81	−1.06	−0.75	−1.22	−1.93	−1.02	−0.91
	1,4-di-σ-2,3π	−1.28	−1.88	−1.13	−0.74	−1.23	−1.90	−1.11	−0.78

Pd_3Ni_1(1 1 1) than on Pd_1Ni_3(1 1 1). By subtraction, the charge transfer (μ_{transf}) contribution was evaluated for each case. Their negative values indicate that adsorptions are governed by stronger donation effects from the molecules to the multilayer materials than back-donation effects (see Table 4). The di-π adsorption modes produce the higher μ_{transf} values, as it was previously found with others adsorbates and other surfaces [45]. The sites with the internal BD geometry less distorted are the sites with higher μ_{transf} values. Interestingly, the μ_{transf} corresponding to the SP calculations of BD/Pd_3Ni_1(1 1 1) are larger than those of BD/ Pd_1Ni_3(1 1 1); in other words, a larger electron transfer from BD to Pd atoms is obtained for the situation of higher decrease of the Pd mm, suggesting that the electron pairing in Pd atoms comes from the above commented BD to Pd electron transfer.

From the electronic point of view, the Pd_3Ni_1(1 1 1) surface presents analogous features as the pure Pd(1 1 1) surface, specifically, the LDOS curves corresponding to the Pd 4*d*-band have similar widths and comparable density of states at Fermi level [31]. Conversely, the Pd_1Ni_3(1 1 1) surface has a widened 4*d*-band (by ~1 eV) and a lower density of states at Fermi level as a consequence of the great reduction of Pd–Pd distance when Pd atoms are deposited on the Ni(1 1 1) surface. In Figs. 3 and 4 are shown the LDOS curves corresponding to BD adsorbed in the 1,2,3,4-tetra-σ site of Pd_1Ni_3(1 1 1) and Pd_3Ni_1(1 1 1) surfaces, respectively, which is the most stable site on both surfaces when the calculations are performed at SP level. For comparison, in different panels are shown the results for both NSP and SP approaches. Looking the NSP results of BD/ Pd_1Ni_3(1 1 1), we observe that a significant coupling of the d_z^2 band of Pd with p_z orbitals of C atoms takes place. The d_z^2 band of Pd broadens, with a concentration of the states at higher binding energy values with respect to the bare bimetallic surface. The displacement of the d_z^2 band center is of ~1.60 eV with respect to the clean surface (−2.40 eV). The coupling between the substrate d_z^2 band and the Cp_z orbitals of the adsorbate produces a large splitting of Cp_z orbitals from ~−7 to ~−5 eV; the states above the Fermi level correspond to the mixing between the d_z^2 band with the antibonding π^* states of BD. The interaction involving the Cp_z orbitals and the d_{yz} band of the Pd atoms also occurs, but its degree is lower with respect to the previous mentioned Cp_z–d_z^2 coupling. The presence of a peak in the LDOS(Cp_z) at ~−7.2 eV corresponds to the former interaction. For the SP results, the better coupling was also obtained between the Cp_z orbitals and d_z^2 band of Pd (Fig. 3b). This band is pushed downward by ~1.2 eV with respect to the clean Pd/Ni surface and a large splitting of the Cp_z orbitals is observed. A peak appears at −6.6 eV, attributed to the interaction of Cp_z orbital with the d_{yz} band. An interesting property is that the unbalance between the spin-up and the spin-down states present in the clean surface practically disappears upon the diene adsorption. This behavior is in agreement with the above commented

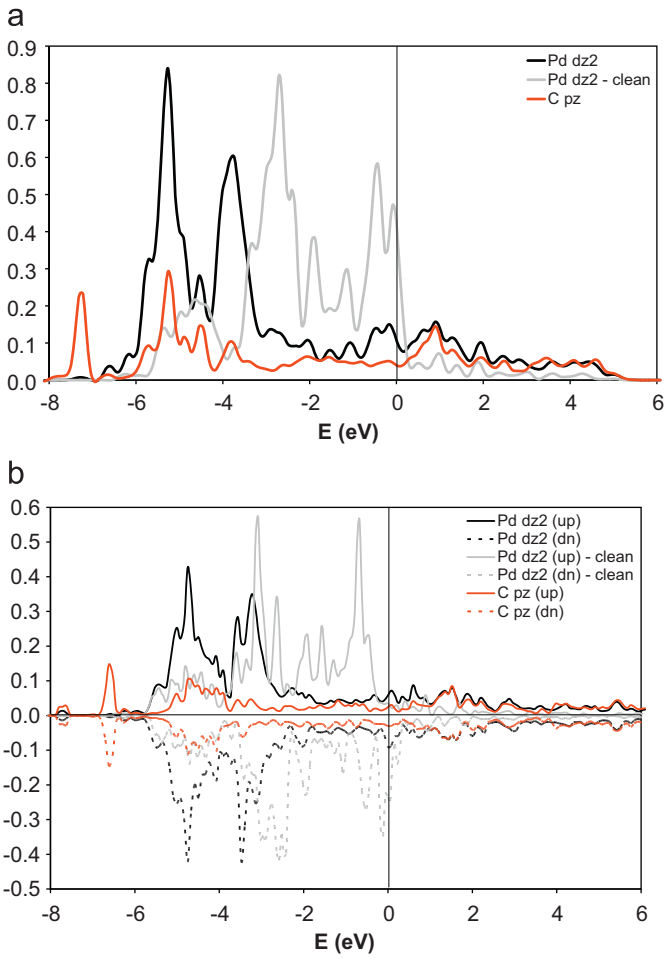

Fig. 3. LDOS of interacting C and Pd atoms for 1,3-butadiene adsorbed on the Pd_1Ni_3 multilayer surface in the 1,2,3,4-tetra-σ site: (a) NSP level of calculation and (b) SP level of calculation.

decrease of the magnetic moment of interacting Pd atoms in the surface.

Looking at the LDOS curves for the BD/Pd_3Ni_1(1 1 1) system surface, we observe again that, at both NSP and SP levels, a stronger coupling of the d_z^2 band is produced with the Cp_z orbitals of BD. As it was observed for clean Pd/Ni surfaces, the energy range covered by the 4*d*-band of Pd in BD/Pd_3Ni_1(1 1 1) is reduced by ~1.0 eV with respect to BD/Pd_1Ni_3(1 1 1) [31]. The BD adsorption produces a 4*d*-band downshift of approximately −1.5 eV with respect to the

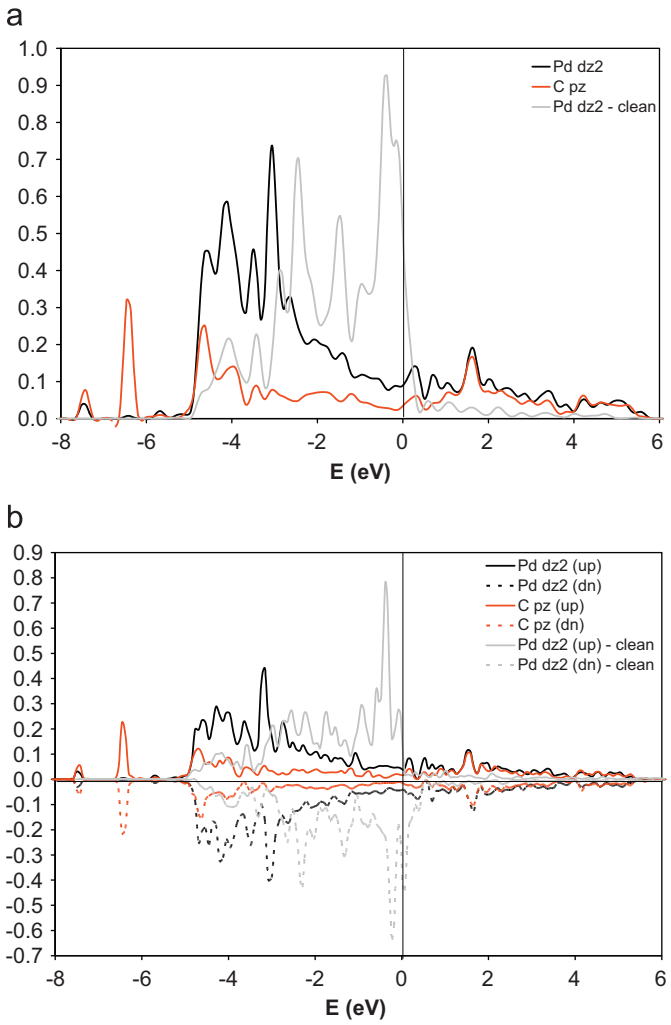

Fig. 4. LDOS of interacting C and Pd atoms for 1,3-butadiene adsorbed on the Pd_3Ni_1 multilayer surface in the 1,2,3,4-tetra-σ site: (a) NSP level of calculation and (b) SP level of calculation.

free bimetallic surface (− 1.86 eV). The Cp_z orbitals present a large splitting from ∼ − 5 eV to ∼ − 6 eV, with the states above the Fermi level composed by the antibonding π^* states of BD. The peak at − 6.5 eV corresponds to the interaction of the Cp_z orbitals with the d_{yz} bands. Specifically, from the LDOS obtained at the SP level, we observe that the unbalance between the spin-up and spin-down states after the diene adsorption decreases considerably but does not disappear. This property is in agreement with the values of the mm of interacting Pd atoms.

3.2. Adsorption of butene isomers on Pd/Ni surfaces

The adsorption of butene isomers, i.e., *cis*/*trans*-2-butene and 1-butene were also studied on both Pd/Ni surfaces. The adsorption energies and geometric parameters are summarized in Tables 1 and 2. The di-σ adsorption mode is the most stable for the butene isomers and only the results for this mode are presented. As it was reported in previous works [13,14,45], the geometries of the isomers were modified with a bending of the hydrogen or alkyl groups away from the surface. In all the cases, the original planarity of the free molecules is broken. In these adsorbates, the C=C double bond is significantly longer than in the free molecule, with a lengthening of nearly 0.1 Å. The internal geometry of the butenes is unaffected when the bimetallic surface is changed and when a different level of the calculation (NSP/SP) is carried out. The C–Pd bonds are slightly longer on Pd_1Ni_3(1 1 1) than Pd_3Ni_1(1 1 1), as it was observed for BD.

The adsorption energies of three butenes strongly depend of the surface composition. Their values are significantly higher on Pd_3Ni_1(1 1 1) than on Pd_1Ni_3(1 1 1) (∼50%). For both surfaces and both calculation levels, the stability of the isomers has the following order: 1-butene > *cis*-2-butene > *trans*-2-butene. The percentage of the *cis*/*trans*-2-butenes destabilization with respect to the 1-butene isomer is more evident when they are adsorbed on the Pd_1Ni_3(1 1 1) surface, being these differences even more marked at the SP level.

The 1-butene stability adsorbed on Pd/Ni surfaces is always lower than the BD adsorbed on its most preferred adsorption mode. The adsorption energy differences between them are more marked on Pd_3Ni_1(1 1 1), i.e., 0.72 eV for Pd_3Ni_1(1 1 1) and 0.18 eV for Pd_1Ni_3(1 1 1). This behavior is the same at both NSP and SP levels. On the other hand, previous theoretical studies performed by Sautet et al. [14] and Mittendorfer et al. [13] for these molecules on pure Pd(1 1 1) showed an adsorption energy difference of 0.82 and 0.96 eV, respectively.

In view of these results, it is possible to affirm that the BD and 1-butene adsorb more strongly on pure monometallic Pd surfaces than on Pd–Ni bimetallic surfaces and that this reduced adsorption capability is related to the strain present in the surfaces of Pd–Ni multilayers. Accordingly, this reduced adsorption capability could account for the increased reactivity of these systems. Indeed, the growing of one and three monolayers of Pd deposited pseudomorphically on the Ni(1 1 1) surface reduces the stability of these chemisorbed species. The experimental data for the BD catalytic hydrogenation on a Pd_8Ni_{92}(1 1 1) alloy showed higher activity than on monometallic Pd(1 1 1) [20,46]. In this alloy, the segregation of Pd on the surface is up to quasi-complete superficial monolayer (76%) with (1 1 1) orientation. Subsequent studies performed on 1–3 monolayers of Pd deposited epitaxially on Ni(1 1 1) showed that these systems were more active than the bimetallic alloy [47]. One Pd monolayer on Ni(1 1 1) surface was even more reactive than the catalyst with three monolayers of Pd. For both catalysts, the selectivity towards butenes was 100% up to quasi-complete conversion of butadiene.

In a previous theoretical work [27] the ethylene hydrogenation on the Pd–Ni bimetallic was investigated in order to understand the high activity of the structured catalyst obtained by deposition of Pd on Ni(1 1 0). The model of the Pd–Ni(1 1 0) surface was built taking into account a previous experimental study where evidences for the reconstruction of the Pd/Ni interface are given [48,49]. The adsorption energies of ethylene on this strained and reconstructed Pd surface are lower than those obtained on a pure monometallic Pd(1 1 0). This behavior is similar to our results, where the Pd_1Ni_3(1 1 1) slab shows the lowest adsorption energies for BD.

On the other hand, it is important to consider that for the catalytic hydrogenation of an alkene, this species as well as atomic hydrogen must be adsorbed on the surface of the catalyst. Interesting results were reported by Valcarcel et al. [50], obtaining a greater activity on Pd–Ni catalysts in comparison with Pd catalysts, specially, at low H_2 pressures. The rate-law obeyed in each case depends of the partial order in H_2 pressure; this partial order is much higher for fresh Pd than for fresh Pd–Ni catalysts. Besides, the structure of the surface is an essential issue to be taken into account for the dissolution of hydrogen in the bulk of the metals. The opened structures, like Pd(1 0 0) or Pd(1 1 0) [51–53], occlude more H than the closed structures. This phenomenon was also observed by Valcarcel et al. [50] in the case of monometallic Pd surfaces, while the Pd–Ni alloy presented a lower hydrogen occlusion. In the last system, Ni essentially acted as a support for Pd and prevented the diffusion of hydrogen into the bulk; crystalline Ni is known to absorb much less hydrogen than Pd

under mild conditions [54]. On the other hand, in the case of clean Pd crystals, the H dissolution competes with surface reactions and the catalytic activity increases when the subsurface Pd is enriched with hydrogen. The Pd–Ni overlayer catalyst behaves as the nanoparticles of Pd, maintaining the hydrogen atoms in the near-surface region.

Summarizing, the chemisorption of these alkene species is greatly affected by the stress present in the Pd overlayers induced by the Ni(1 1 1) substrate. On the Pd_1Ni_3(1 1 1) surface, both BD and 1-butene have the lowest adsorption energies at SP level, as a consequence of the large strained surface. This result could be associated to the fact that the Pd–Ni(1 1 1) overlayer shows the highest activity [27]. To our knowledge, no experimental results of selectivity of bimetallic multilayer surfaces were reported. The noticeable lower adsorption strength of 1-butene on Pd_1Ni_3(1 1 1) would imply that as soon as it is produced is desorbed from the surface, leading to a higher selectivity with respect to Pd_3Ni_1(1 1 1) and Pd(1 1 1) [13,55].

4. Conclusions

The adsorption energies and adsorption geometries of BD and butene isomers were obtained on two Pd–Ni multilayer slabs with different compositions: Pd_1Ni_3(1 1 1) and Pd_3Ni_1(1 1 1), taking into consideration the ferromagnetic property of Ni metal. The calculations were performed at both NSP and SP levels. The most preferred adsorption mode of BD depends on the substrate composition and whether the NSP or SP calculations were realized. For the Pd_1Ni_3(1 1 1) surface, the di-π-cis and 1,2,3,4-tetra-σ adsorption modes are the most stables at NSP and SP levels, respectively. On the other hand, the 1,2,3,4-tetra-σ site was the most - stable adsorption mode for Pd_3Ni_1(1 1 1) with both theoretical approaches. In all the cases, the magnitude of the adsorption energies of BD and butene isomers is higher on the surface with greater Pd contents. This behavior could be associated with the similar electronic structure of Pd_3Ni_1(1 1 1) and pure Pd(1 1 1). The SP calculations show that the BD molecule decreases significantly the magnetic moment of Pd atoms of the top layer; this effect being more noticeable when the BD molecule adsorbs strongly at the bimetallic surface and a larger electron transfer is produced from BD to the Pd atoms.

Analyzing the adsorption energies of the most stable adsorption mode for BD and for 1-butene on these multilayer Pd/Ni surfaces, it is possible to affirm their lower chemisorption on the Pd–Ni bimetallic surfaces than on pure Pd(1 1 1). This reduced adsorption can be associated with the stress induced in the superficial layers of Pd. Besides, the BD hydrogenation on Pd_1Ni_3(1 1 1) surface could present higher selectivity towards 1-butene than Pd_3Ni_1(1 1 1) and pure Pd(1 1 1), due to its smaller adsorption strength. Preliminary results of the hydrogenation pathways show promissory results for this bimetallic catalyst.

Acknowledgments

The authors thank the financial support from the Consejo Nacional de Investigaciones Científicas y Técnicas (CONICET), The Agencia de Promoción Científica y Tecnológica (ANPCyT) and the Departamento de Física de la Universidad Nacional del Sur (UNS).

References

[1] G.C. Bond, Metal-Catalyzed Reactions of Hydrocarbons, Springer, New York,, 2005.
[2] B. Chen, U. Dingerdissen, J.G.E. Krauter, H.G.J. Lansink Rotgerink, K. Möbus, D.J. Ostgard, P. Panster, T.H. Riermeier, S. Seebald, T. Tacke, H. Trauthwein, Appl. Catal. A 280 (2005) 17.
[3] A.J. Wright, A.L. Mihele, L.L. Diosady, Food Res. Int. 36 (2003) 797.
[4] A.J. Wright, A. Wong, L.L. Diosady, Food Res. Int. 36 (2003) 1069.
[5] Sarkany, Z. Zsoldos, B. Furlong, J.W. Hightower, L. Guczi, J. Catal. 141 (1993) 566.
[6] Sarkany, Z. Zsoldos, Gy. Stefler, J.W. Hightower, L. Guczi, J. Catal. 157 (1995) 179.
[7] P. Hermann, B. Tardy, D. Simon, J.M. Guigner, B. Bigot, J.C. Bertolini, Surf. Sci. 307–309 (1994) 422.
[8] T. Ouchaib, J. Massadier, A. Renouprez, J. Catal. 119 (1989) 517.
[9] Z. Dobrovolná, P. KaČer, L. Červený, J. Molec. Catal. A: Chemical 3 (1998) 279.
[10] G. Tourillon, A. Cassuto, Y. Jugnet, J. Massadier, J.C. Bertolini, J. Chem. Soc. Faraday Trans. 92 (1996) 4835.
[11] C. Yoon, M.X. Yang, G.A. Somorjai, Catal. Lett. 46 (1997) 37.
[12] J.C. Bertolini, A. Cassuto, Y. Jugnet, J. Massardier, B. Tardy, G. Tourillon, Surf. Sci. 349 (1996) 88.
[13] F. Mittendorfer, C. Thomazeau, P. Raybaud, H. Toulhoat, J. Phys. Chem. B 107 (2003) 12287.
[14] A. Valcárcel, A. Clotet, J.M. Ricart, F. Delbecq, P. Sautet, Surf. Sci. 549 (2004) 121.
[15] J. Silvestre-Albero, G. Rupprechter, H.-J. Freund, Chem. Commun. (2006) 80.
[16] J. Silvestre-Albero, G. Rupprechter, H.-J. Freund, J. Catal. 240 (2006) 58.
[17] L. Piccolo, A. Valcarcel, M. Bausach, C. Thomazeau, D. Uzio, G. Berhault, Phys. Chem. Chem. Phys. 10 (2008) 5504.
[18] L. Piccolo, A. Piednoir, J.C. Bertolini, Surf. Sci. 592 (2005) 169.
[19] P. Miegge, J.L. Rousset, B. Tardy, J. Massardier, J.C. Bertolini, J. Catal. 149 (1994) 404.
[20] A.C. Michel, L. Lianos, J.L. Rousset, P. Delichère, N.S. Prakash, J. Massardier, Y. Jugnet, J.C. Bertolini, Surf. Sci. 416 (1998) 288.
[21] P. Hermann, J.M. Guigner, B. Tardy, Y. Jugnet, D. Simon, J.C. Bertolini, J. Catal. 163 (1996) 169.
[22] M. Abel, Y. Robach, J.C. Bertolini, L. Porte, Surf. Sci. 454–456 (2000) 1.
[23] M.C. Saint-Lager, Y. Jugnet, P. Dolle, L. Piccolo, R. Baudoing-Savois, J.C. Bertolini, A. Bailly, O. Robach, C. Walker, S. Ferrer, Surf. Sci. 587 (2005) 229.
[24] M.F. Carazzolle, S.S. Maluf, A. de Siervo, P.A.P. Nascente, R. Landers, G.G. Kleiman, Surf. Sci. 600 (2006) 2268.
[25] P.A.P. Nascente, M.F. Carazzolle, A. de Siervo, S.S. Maluf, R. Landers, G.G. Kleiman, J. Mol. Catal. A 281 (2008) 3.
[26] P. Hermann, D. Simon, P. Sautet, B. Bigot, J. Catal. 167 (1997) 33.
[27] J.-S. Filhol, D. Simon, P. Sautet, J. Am. Chem. Soc. 126 (2004) 3228.
[28] Y.S. Shi, M.F. Wang, D. Qian, G.S. Dong, X.F. Jin, Ding-Sheng Wang, J. Magn. Magn. Mater. 277 (2004) 71.
[29] Z.B. Tang, C.S. Tian, L.F. Yin, G.S. Dong, Xiaofeng Jin, J. Magn. Magn. Mater. 310 (2007) 1804.
[30] A. Valcarcel, D. Loffreda, F. Delbecq, L. Piccolo, Phys. Rev. B 76 (2007) 125406.
[31] G. Gómez, G.F. Cabeza, P.G. Belelli, J. Magn. Magn. Mater. 321 (2009) 3478.
[32] G. Kresse, J. Hafner, Phys. Rev. B 47 (1993) 558.
[33] G. Kresse, J. Hafner, Phys. Rev. B 48 (1993) 13115.
[34] G. Kresse, J. Hafner, Phys. Rev. B 49 (1994) 14251.
[35] J.P. Perdew, J.A. Chevary, S.H. Vosko, K.A. Jackson, M.R. Pederson, D.J. Singh, C. Fiolhais, Phys. Rev. B 46 (1992) 6671.
[36] J.P. Perdew, J.A. Chevary, S.H. Vosko, K.A. Jackson, M.R. Pederson, D.J. Singh, C. Fiolhais, Phys. Rev. B 48 (1993) 4978.
[37] P. Blochl, Phys. Rev. B 50 (1994) 17953.
[38] G. Kresse, D. Joubert, Phys. Rev. B 59 (1999) 1758.
[39] H.J. Monkhorst, J.D. Pack, Phys. Rev. B 13 (1976) 5188.
[40] M. Methfessel, A.T. Paxton, Phys. Rev. B 40 (1989) 3616.
[41] P.C. Rusu, G. Brocks, Phys. Rev. B 74 (2006) 073414.
[42] Q. Ge, S.J. Jenkins, D.A. King, Chem. Phys. Lett. 327 (2000) 125.
[43] M.B. Knickelbein, J. Chem. Phys. 115 (2001) 1983.
[44] A. Hammoudeh, J. Loboda-Cackovic, M.S. Mousa, J.H. Block, Vacuum 48 (1997) 187.
[45] P.G. Belelli, R.M. Ferullo, N.J. Castellani, Surf. Sci. 604 (2010) 386–395.
[46] L.J. Shorthouse, Y. Jugnet, J.C. Bertolini, Catal. Today 70 (2001) 33.
[47] J.C. Bertolini, Appl. Catal. A 191 (2000) 15.
[48] J.-S. Filhol, D. Simon, P. Sautet, Phys. Rev. B 64 (2001) 085412.
[49] J.-S. Filhol, D. Simon, P. Sautet, Surf. Sci. 472 (2001) L139.
[50] A. Valcarcel, F. Morfin, L. Piccolo, J. Catal. 263 (2009) 315.
[51] J. Quinn, Y.S. Li, D. Tian, H. Li, F. Jona, P.M. Marcus, Phys. Rev. B 42 (1990) 11348.
[52] J. Burchhardt, E. Lundgren, M.M. Nielsen, J.N. Andersen, D.L. Adams, Surf. Rev. Lett. 3 (1996) 1339.
[53] S.H. Kim, H.L. Meyerheim, J. Barthel, J. Kirschner, J. Seo, J.-S. Kim, Phys. Rev. B 71 (2005) 205418.
[54] B. Baranowski, S.M. Filipek, J. Alloys Compd. 404 (2005) 2 and references therein.
[55] H.H. Hwu, J. Eng Jr., J.G. Chen, J. Am. Chem. Soc. 124 (2002) 702.